Biochemical Engineering Journal 97 (2015) 125–131

Contents lists available at ScienceDirect

Biochemical Engineering Journal

journal homepage: www.elsevier.com/locate/bej

Regular article

Interaction of mercury and copper on papain and their combined inhibitive determination

Xue-Ying Liu [a,b], Hong-Yan Zeng [a,*], Meng-Chen Liao [a], Bo Feng [a,*], Bi Foua Claude Alain Gohi [a]

[a] Biotechnology Institute, College of Chemical Engineering, Xiangtan University, Xiangtan 411105, Hunan, China
[b] Hunan Key Laboratory of Green Packaging and Application of Biological Nanotechnology, Hunan University of Technology, Zhuzhou 412007, China

ARTICLE INFO

Article history:
Received 14 October 2014
Received in revised form
19 December 2014
Accepted 7 January 2015
Available online 8 January 2015

Keywords:
Protease
Biocatalysis
Enzyme activity
Mercury ion
Copper ion
Kinetic parameters

ABSTRACT

Influence and interaction of mercury ion (Hg^{2+}) and copper ion (Cu^{2+}) on papain activity in casein hydrolysis were investigated. Single Hg^{2+} or Cu^{2+} at low concentrations induced an increase in papain activity, but decreased it at high concentrations, confirming a typical hormesis phenomenon. The interaction of Hg^{2+} and Cu^{2+} at various concentration combinations showed that the binary interaction of 10^{-8} mol/L Cu^{2+} and 10^{-6} mol/L Hg^{2+} (Binary union S) buffer was of synergistic nature, while 10^{-4} mol/L Cu^{2+} and 10^{-4} mol/L Hg^{2+} (Binary union I) buffer was of competitive inhibition. The conformational changes in papain structure due to the interaction of binary metal ions were studied by ATR-FTIR, UV–vis and intrinsic fluorescence spectroscopies, also the changes of papain catalytic behavior were studied through kinetic analysis. Decreasing of α-helix content with increasing in intermolecular β-sheet aggregates content in Binary union I buffer resulted in an inactivation of papain activity by 57.2% and lower affinity for casein. On the contrary, papain activity increased with α-helix content increasing and intermolecular β-sheet aggregates content decreasing in Binary union S buffer. The competitive interaction between Cu^{2+} and Hg^{2+} on papain activity was found at higher concentrations ($\geq 10^{-4}$ mol/L), and the inhibition of the binary metal ions on papain was of a noncompetitive type.

1. Introduction

Due to incessant industrial development, heavy metal contaminants have been introduced into water environments and become an increasingly serious social problem. Owing to their bioaccumulation and non-degradability, heavy metals pose a serious pollution hazard to the aqueous environment [3,4,7,20]. Certain metal ions are highly toxic, and the determination of trace toxic heavy metals in water environments has become highly important. Among all of them, Hg^{2+} has attracted the most attention due to its strong toxicity and increasing level of its extended use in industrial processes [12]. In order to evaluate the toxicity, bioavailability, bioaccumulation and transport of the heavy metal elements more readily, sensitive analytical procedures are required for detection [2]. Numerous enzymes have been utilized for heavy metal detection, for enzyme activity is an indicator of the toxicity of heavy metals and other pollutants [1,11,15,22]. The aforementioned studies were mostly concentrated on the effect of a single heavy metal ion. However, contaminated systems usually contain various heavy metals rather than a single one in the real environment. As a consequence, enzymes are exposed to multiple metal ions system. Still, most enzyme biosensors detect heavy metals in contaminated water and derive single-substance toxicity data from single-substance criteria, but neglecting the interaction effects among the mixture. So, the detecting methods for the presence of two or more ions are thus urgently needed [5].

Papain is a highly stable enzyme, one of the proteolytic enzymes of papaya latex [16]. Papain has been widely used as biosensors for its wide pH span for optimum activity, high sensitivity, temperature stability, low price, and short response time. But few influence assays on mixed heavy metal ions based on papain have been reported, particularly on inhibition [20]. Metal ions such as Cu^{2+}, Hg^{2+}, Zn^{2+}, and Pd^{2+} were found not only binding to papain but also inhibiting its activity partly or completely. The IC_{50} of Hg^{2+}, Ag^{2+}, Pb^{2+} and Zn^{2+} were 0.39, 0.40, 2.16 and 2.11 mg/L, respectively, while for Cu^{2+} and Cd^{2+}, the limit of quantitation were 0.004 and 0.1 mg/L, respectively [20].

In the preliminary stage of our work, we observed that the interactive effect of the two mixed metal ions on papain activity was

* Corresponding authors. Tel.: +86 731 58298175; fax: +86 731 58298167.
E-mail addresses: hongyanzeng99@hotmail.com (H.-Y. Zeng), fengbo@xtu.edu.cn (B. Feng).

http://dx.doi.org/10.1016/j.bej.2015.01.001
1369-703X/

different from that of single Hg^{2+} and Cu^{2+}, while the inactivation of papain activity was about 58% for Cu^{2+} and nearly 100% for Hg^{2+}. The inactivation mechanism affected by the binary ions (Hg^{2+} & Cu^{2+}) was still not clearly understood. The principal aim of this present work was to evaluate the combined effect of Hg^{2+} and Cu^{2+} on papain activity and structure. The ATR-FTIR, UV–vis intrinsic fluorescence spectroscopies and kinetics analysis were used to investigate the structure-function relationship in the presence of the binary ions.

2. Materials and methods

2.1. Enzyme and regents

Papain (EC3.4.22.2, ≥99%), bovine serum albumin (BSA), tyrosine and casein were purchased from Sigma–Aldrich Company Ltd. All other reagents used were of analytical grade and used without further purification. All solutions were prepared with redistilled and ion-free water.

2.2. Effect of single metal ion on papain activity

Papain solution (1.0 mg/mL) was obtained by dissolving the enzyme in Tris–HCl buffer (0.1 mol/L, pH 7.0). Stock solution of $HgCl_2$ (0.1 mol/L) and $CuCl_2$ (0.1 mol/L) were prepared in the Tris–HCl buffer and diluted into the concentrations varied from 10^{-10} to 10^{-2} mol/L for papain activity assays. Firstly, papain solution (1 mL) was added into the buffer (1 mL) of different metal ion concentrations at 40 °C, secondly casein solution (3.0 mL, 20.0 mg/mL) was added into the mixture 10 min later. The reaction was carried out at 40 °C for 30 min and then stopped by 2.0 mL trichloroacetic acid (TCA). The activity of papain was determined by a Hitachi U-2001 spectrophotometer at 275 nm. One unit of enzyme activity (U) was defined as 1 μg tyrosine formed per minute at 40 °C and pH 7.0. The relative activity (%) was the ratio of the enzyme activity in the Tris–HCl buffer with different Hg^{2+} or Cu^{2+} concentrations to the corresponding enzyme activity without Hg^{2+} or Cu^{2+}. All the experiments were carried out at least three experiments in each experimental group and the average number was employed as the statistical analysis indicator.

2.3. Effect of the binary ions on papain activity

In order to determine the interactive effect of Hg^{2+} and Cu^{2+} ions on papain activity, the assay was performed by incubating the papain in the binary ions buffer. The buffer was prepared by mixing equal volume of Hg^{2+} and Cu^{2+} buffers at different concentration. Papain activity in the presence of the mixed metal ions was also monitored as described above.

2.4. ATR-FTIR, UV–vis and intrinsic fluorescence spectroscopies

ATR-FTIR spectra of the samples in the ATR cells were recorded on PE Spectrum One B instrument. Background was subtracted using the Opus software. Curve fitting was then performed using Origin 9.0 and PeakFit v4.12 software. The absorbance spectra of the samples were recorded by a Hitachi UV9100 spectrophotometer. The range of wavelength is 190–500 nm. The tryptophan (Trp) fluorescence spectra were recorded by a PE LS55 spectrofluorimeter at 30 °C. The emission spectra were recorded in the range of 300 ~ 410 nm at 500 nm/min, 10 s after excitation, keeping the excitation constant at 288 nm, with slit widths of 5 nm for excitation and emission. Tryptophan ethyl ester was used as internal standard to correct an inner filter effect. The blank spectrum without enzyme was subtracted from the sample spectra.

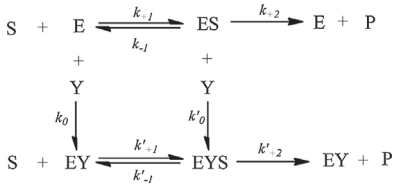

Scheme 1. The irreversible reaction mechanism of the binary metal ions.

The papain (0.5 mg/mL) was equilibrated in the solutions with the binary ions of 10^{-8} mol/L Cu^{2+} + 10^{-6} mol/L Hg^{2+} (Binary union S) and 10^{-4} mol/L Cu^{2+} + 10^{-4} mol/L Hg^{2+} (Binary union I) under 25 °C for 10 min, respectively, and then centrifuged at 3000 rpm (equal to *g* value 800) for 4 min. The papain without any metal ions treated was used as the control. The supernatant was used for ATR-FTIR, UV–vis and fluorescence spectral measurements. Triplicate samples were analyzed and the data obtained from the triplicate runs were averaged and used as the final result.

2.5. Kinetic measurements

The kinetic model of substrate reaction during irreversible modification of enzyme activity described by Zhao and Tsou was used to study the kinetics of casein hydrolysis by papain with the binary metal ions [24]. The reaction mechanism was considered in Scheme 1, where *E*, *S*, *P* and *Y* represent papain, substrate casein, product tyrosine and the binary ions, respectively. EY, ES and EYS were the respective complexes.

As was usual the case, [*S*] » [E_0] and that the modification reactions were relatively slow compared with the setup of the steady-state of the enzymatic reaction. The product formation can be written as:

$$[P]_t = v't + \frac{v - v'}{A}(1 - e^{-At}) \quad (1)$$

$$A = \frac{k_0 K_m + k_0' [S]}{K_m + [S]} \quad (2)$$

where $[P]_t$ was the concentration of the product formed at time *t*. *A* was the apparent rate constants. [*S*] was the concentration of casein. v and v' were the reaction velocities of reaction in the absence and presence of the binary ions at time *t*, respectively. K_m and K_m' were the Michaelis constants. k_0 and k_0' were the dissociation constants for the modifier with different forms of the enzyme, respectively. V_m and V_m' were maximum reaction velocities. When $v > v'$, the binary metal ions modifier was an activator. When $v < v'$, the modifier binary ions was an inhibitor. When *t* was sufficiently long, the curves become straight lines and the product concentration was written as [P_e]:

$$\frac{1}{[P_e]} = \frac{k_0 \cdot K_m}{V_m} \cdot \frac{1}{[S]} + \frac{k_0'}{V_m} \quad (3)$$

3. Results and discussion

3.1. Effect of single metal ion on papain activity

The effects of different concentrations of Hg^{2+} or Cu^{2+} on papain activity were investigated and typical low-dose stimulation and high-dose inhibition (hormesis) was shown in Fig. 1. Hg^{2+} inhibited papain activity with a relative activity of 6.78% when Hg^{2+} concentration was ≥10^{-4} mol/L, but it was observed that stimulation of papain activity could occur at 10^{-6} mol/L of Hg^{2+} concentration and displayed the highest relative activity of 111.10%. There was no significant difference in papain activity, exposing to $10^{-10} \sim 10^{-7}$ of Hg^{2+}. At the same time, the maximum of 58.10% inhibition by Cu^{2+} (41.90% relative activity) was at 10^{-4} mol/L, and stimulation with

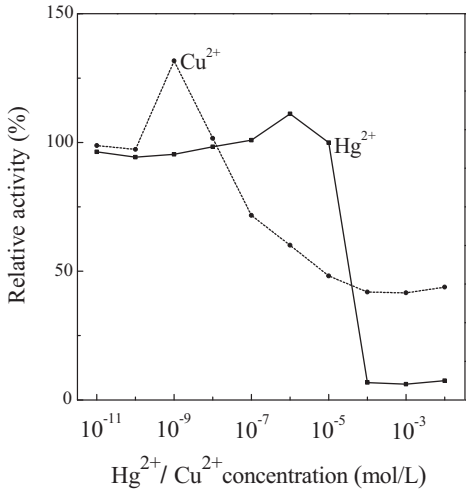

Fig. 1. Effect of single metal ion on papain activity. ·····: Cu^{2+}; —Hg^{2+}.

about 131.70% relative activity at 10^{-9} mol/L. There was no effect of Cu^{2+} below 10^{-10} mol/L on papain activity. In order to see the effect of chloride anion, the effect of KCl on papain activity was checked and there was no change in papain activity (data not shown). Thus the change in the activity observed was mainly due to the Hg^{2+}/or Cu^{2+}.

3.2. Effect of binary ions on papain activity

In order to investigate the interactive effect of the binary ions on papain activity, the activity of papain at each testing combination of Hg^{2+} and Cu^{2+} was determined, and the binary ions range of 10^{-9}–10^{-3} mol/L was based on above results (Fig. 1). The results were listed in Table 1. The maximum stimulation was 180.80% relative activity when exposed in Binary union S buffer, showing that the binary ions enhanced the relative activity by 49.10% comparing with the maximum activation of single Hg^{2+} or Cu^{2+}. On the other hand, the maximum inhibition was only 42.8% relative activity in the presence of Binary union I, which was obviously higher than that of single Hg^{2+} at 10^{-4} mol/L on the relative activity (6.78%). Cu^{2+} was found to suppress the inhibitory effect of Hg^{2+}, and interact antagonistically at most test levels except at combinations of low concentrations of both $10^{-9} \sim 10^{-5}$ mol/L for Cu^{2+} and $10^{-6} \sim 10^{-5}$ mol/L for Hg^{2+}, at which they interacted additively. Results of those experiments ranged from antagonistic to synergistic responses, the overall trend was the addition of Cu^{2+} reduced toxicities of Hg^{2+} on papain. The negative interaction between the two metal ions was probably the result of the competition between

Table 1
Effect of the binary metal ions on papain activity at different test combinations.

	(Concentration unit: mol/L, papain activity: %)						
$C_{Cu^{2+}}$	10^{-3}	10^{-4}	10^{-5}	10^{-6}	10^{-7}	10^{-8}	10^{-9}
Relativeactivity(%) $C_{Hg^{2+}}$							
10^{-3}	40.8	41.1	42.8	41.1	42.6	42.5	43.0
10^{-4}	43.4	42.8	42.3	41.9	42.6	41.9	42.1
10^{-5}	42.1	55.1	103.5	112.3	148.3	151.2	146.2
10^{-6}	76.6	90.6	124.5	176.5	170.0	180.8	172.9
10^{-7}	42.3	44.4	47.4	66.1	67.0	82.7	92.6
10^{-8}	41.1	44.4	47.8	66.7	63.9	95.4	88.2
10^{-9}	40.9	44.2	63.6	62.0	64.8	84.5	78.9

The reactions were performed at 40 °C, pH 7.0 for 30 min, 1.0 mg/mL papain Tris–HCl solution in different concentration combinations of Hg^{2+} and Cu^{2+} ions. Every group test was run three times and the mean values were used as the final test results.

Hg^{2+} and Cu^{2+} for the binding sites in papain. One of the most interesting findings was that Cu^{2+} showed various degrees of inhibition on papain activity below 10^{-7} mol/L Hg^{2+}, suggesting that papain was more sensitive to the binary ions. Given all that, the binary ions were more effective in affecting papain activity than single Hg^{2+} or Cu^{2+}, though papain activity was entirely inhibited by Hg^{2+} at 10^{-4} mol/L. Papain could be adapted to analysis of the binary ions with a low detection limit (10^{-4} mol/L), a large analytical range and a short response time. According to the results of the experiment on papain activity, the Binary union S and I were chosen to investigate the interactions between the binary ions and papain activity & structure.

3.3. Influence of binary metal ions on papain secondary structure

It was possible that the change in papain activity observed in the binary ions buffer might be due to secondary structure change of papain. The changes in papain secondary structure were determined by ATR-FTIR, UV–vis and fluorescence spectroscopies in the presence of the Binary union S and Binary union I, respectively.

3.3.1. Fluorescence spectroscopy

Fluorescence spectroscopy was used to investigate the perturbation of Trp residues in papain as a result of the binary ions interaction with papain and the fluorescence emission spectra of the samples were shown in Fig. 2A. All the samples showed typical Trp peak excited at about 342 nm and the fluorescence was mainly due to the presence of five Trp residues in papain [13], and the maximum emission of the control was at 344 nm (Fig. 2A (a)). Upon interaction of papain with binary union S, the maximum fluorescence emission appeared a blue shift (6 nm, Fig. 2A (b)) and decrease in intensity compared with the control. This blue-shift could be attributed to the conformational changes in the vicinity of surface-exposed Trp residues, presumably because of internalization into a more hydrophobic environment. And the decreased fluorescence intensities also indicated burying of the surface-exposed Trp molecules in the interior of the protein. In case of the Binary union I, the marked decrease in intensity and a red shift of 3 nm in the emission maximum were found (Fig. 2A (c)). It might be deduced that the internalized Trp residues in native state got partially exposed from a hydrophobic to a hydrophilic environment leading to partial unfolding of the molecule. In the last case, the Trp residues were buried inside a more polar protein surrounding, resulting in an inactive enzyme. All these data clearly suggested that the structural alteration of papain exposed in binary ions buffers induced the microenvironment change of the Trp residues. The pattern of the two ions bounded to papain and located at papain molecular interface/protein surface, this might be analogous to the bound pattern of cadmium to saru-actinidin [23]. Papaya protease omega (ppΩ) and saru-actinidin have homologous overall conformation to papain. ppΩ has a mercury atom bound to its active site cysteine, and the NZ atom of Lys64 is 2.88 Å from the mercury atom of a symmetry-related molecule and this contact may be important in determining the arrangement of molecules and hence the space group [18].

3.3.2. UV–vis spectroscopy

Papain has 212 amino acid residues and consists of two domains, with the active site in the groove between the domains. One consists of 10–111 and 208–212 residues (L-domain) containing mainly α-helix and another consists of the remaining residues (R-domain) with a large amount of β-sheet. It has 5 Trp residues, 2 of which are located in the α-helix segments of the L-domain, and 3 (Trp 7 in the β-sheet, Trp 177 and Trp 181 in the coil region) in the R-domain [6,9]. UV–vis absorption measurement was a simple

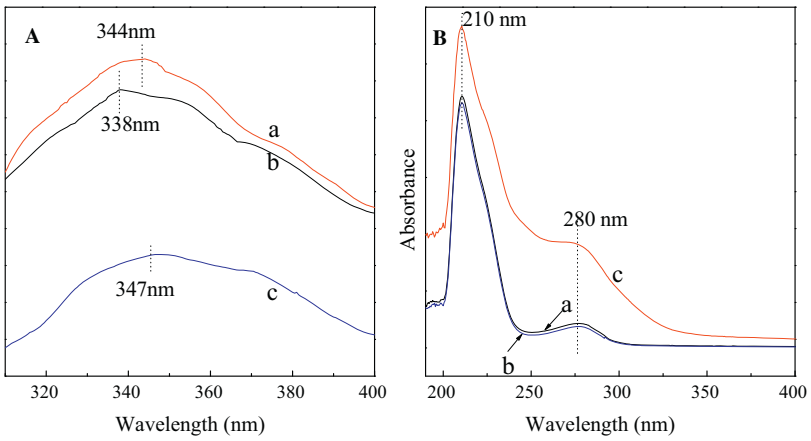

Fig. 2. Fluorescence emissionspectra (A) and UV–vis spectra (B) of the papain samples exposed to Binary union S and I buffer. (a): Control; (b): Binary union S and (c): Binary union I.

and applicable method to study the binding of small molecule substances to protein, which was used as a sensitive measure of subtle changes in protein structure. The UV absorption spectra of papain and papain-binary ions complexes were investigated and the result was shown in Fig. 2B. All the samples similarly displayed the dual absorbance spectra, a strong absorbance with a peak at 210 nm and a broad band centered around 280 nm, where a weak $n \rightarrow \pi^*$ electronic transition occurred at 210 nm for α-helix structure while a higher frequency $\pi \rightarrow \pi^*$ electronic transition at 280 nm for Trp residues [8,14,19]. Clearly, the UV absorption intensity of papain changed with the variation of the binary ions concentration, but its shape almost kept in the same. Comparing with the control, shift of the maximum peak position of papain-binary ions complexes at about 210 nm indicated that the interaction between the binary ions and papain induced to the change of α-helix structure of papain. Increase of absorption intensity of papain-Binary union I complex in the region of 280 nm showed that interaction of them caused Trp residues to migrate towards the protein surface and increased surface accessibility of Trp. While, the decreased absorption intensity of papain-Binary union S complex at 280 nm could be because of the effect of the Binary union S on papain, as a result of conformational changes in papain structure during the interaction of Binary union S with papain, leading to burying insider a less polar protein surrounding. A similar phenomenon was also found on Trp residues change in fluorescence spectral investigation (Fig. 2A), clearly denoting that the interaction between the binary ions and papain induced a significant structure change which could be attributed to the papain conformation including α-helix structure. In order to obtain more information on the binding of the binary ions to papain, ATR-FTIR was employed to study the conformational change of papain.

3.3.3. ATR-FTIR

Deformation in papain secondary structure led to the change of the protein's native three-dimensional structure wherein the function of the protein could also be altered. ATR-FTIR spectroscopy has been used extensively to study the secondary structure changes of protein. The amide I band ($1700 \sim 1600\,cm^{-1}$) was the most useful for spectroscopic analysis of secondary structure of protein [10]. The original ATR-FTIR spectra of the Binary union S and I samples in the $1800 \sim 900\,cm^{-1}$ region were performed and the components peaks in amide I region were determined by curve fitting method (Fig. S1 and Table 2), which the individual component locations of the secondary structure were assigned according to the methods by earlier studies [17,25]. The obtained analytical result showed that the binary ions buffer had significant influence on the secondary structure of papain. Compared with the control, papain exposed in the Binary union S buffer exhibited the increases of α-helix (from 18.28 to 24.74%) and β-sheet contents (from 22.45 to 28.04%), and decreases of β-turn and random coil contents. Especially, papain showed a decrease in the percentage of intermolecular β-sheet aggregates from 9.68 to 8.89%. However, the α-helix and β-sheet contents of papain decreased to 15.66 and 18.27%, while the intermolecular β-sheet aggregates contents rose to 15.05% in the presence of the Binary union I, but there was only a slight change of β-turn and random coil contents. It could be concluded that the α-helix and intermolecular β-sheet aggregates contents were mainly contribution to the secondary structure change of papain. ATR-FTIR spectra revealed that the structure of papain-binary ions complexes had certain deformation leading to the structural change of papain, which might be considered as a significant factor in affecting its catalytic activity. Of the 2 domains in papain folding structure, L-domain of the native molecule had large α-helix content, while R-domain was mainly β-sheet and a lesser amount of α-helix [6,9,21]. Accompanied by the enhancement of papain catalytic activity (Fig. 1), papain presented a modest increment of α-helix content in the presence of the Binary union S, moreover, slight decrease of intermolecular β-sheet aggregates and random coil contents due to the binding of the Binary union S to papain at low ions concentrations. Nevertheless, exposed in the Binary union I buffer, the binding of the Binary union I to papain decreased α-helix and α-sheet contents and significantly increased the intermolecular β-sheet aggregates content, leading to inactivation of papain. The binding of the binary ions to papain was marked by significant changes of the position in the ATR-FTIR spectra.

With reference to above spectroscopic characterization results, it was confirmed that the papain activity increased with the increase of α-helix content as well as the decrease of intermolecular β-sheet aggregates content, and vice versa. It was important to note that efficient catalytic activity of papain required not only correct active site but also the domain packing properties. Thus these spectroscopic techniques revealed that the conformation change in papain upon the interaction of the binary ionS on papain.

3.4. Kinetic constants

The kinetic parameters, K_m and V_{max}, of the treated papain were calculated from the Lineweaver–Burk and Michaelis–Menten models in presence of the binary metal ions (Binary union S and Binary union I), single Hg^{2+} (10^{-6} and 10^{-4} mol/L) and single Cu^{2+} (10^{-9} and 10^{-4} mol/L) at casein concentrations of 1.0 mg/mL. Lineweaver–Burk reciprocal plots of the samples were shown in

Table 2
Secondary structure assignments and areas in amide I infrared bands of papain samples at Binary union S and I combinations.

Second structure	Binary metal ions concentration (mol/L)					
	Control		Binary union S		Binary union I	
	Peak centers (cm^{-1})	Areas (%)	Peak centers (cm^{-1})	Areas (%)	Peak centers (cm^{-1})	Areas (%)
Intermolecular β-Sheet aggregates	1614	9.68	1614	8.89	1616	15.05
β-Sheet	1627	22.45	1628	28.04	1629	18.27
α-Helix	1655	18.28	1657	24.74	1657	15.66
Random coil	1642	25.22	1643	19.22	1643	26.38
β-Turn	1669	24.37	1670	19.11	1669	24.65
	1683		1682		1683	

The reactions were performed at 40 °C, pH 7.0 for 30 min, 0.5 mg/mL papain Tris–HCl solution was equilibrated in Binary union S and Binary union I under 25 °C for 10 min, and then centrifuged at 800 × *g* for 4 min. The supernatant was used to determine the structure changes of the treated papain. The papain without any metal ions treated was used as the control. All the samples were determined three times and the data obtained from the triplicate runs were averaged and used as the final result.

Fig S2 and Table S1. For the papain exposed in the Binary union S buffer, the V_{max} value increased to 0.195 mg/min comparing with that the control (0.121 mg/min), while K_m decreased from 4.733 to 3.663 mg/mL (Fig S2 A). On the contrary, the V_{max} value of the papain exposed in the Binary union I buffer reduced to 0.067 mg/min, while K_m climbed to 5.163 mg/mL (Fig S2 B). Similar experiments were carried out in the presence of single Hg^{2+} and Cu^{2+}, and the values of K_m were determined, listing in Table S1. The values of K_m indicated the high affinity for casein in the presence of the Binary union S, and low affinity in the Binary union I. Higher K_m values for Hg^{2+} at 10^{-6} and 10^{-4} mol/L than for Cu^{2+} corresponding at 10^{-9} and 10^{-4} mol/L indicated the papain had a lower affinity for the substrate, displaying that the affinity of the papain bound with Hg^{2+} for the substrate was lower than one bound with Cu^{2+}. The papain exposed in the Binary union S buffer had the smallest K_m value, implying that it had the highest affinity for the substrate. The K_m value of the papain exposed in the Binary union I was similar to the one with Cu^{2+} at 10^{-4} mol/L, but much higher than with Hg^{2+} at 10^{-4} mol/L, indicating that addition of Cu^{2+} blocked the inhibition of Hg^{2+} on papain. The result showed that the Binary union I was able to weaken the affinity for the substrate by decreasing α-helix content and enhancing intermolecular β-sheet aggregates content.

3.5. Kinetics properties of papain in the presence of Hg^{2+}

The time course of hydrolysis of casein in different binary ions concentrations was shown in Fig. 3. For the substrate hydrolysis in the presence of $Hg^{2+} + Cu^{2+}$, the rate increased with increasing casein concentration, while the slope of the asymptote increased with increasing casein concentration. The reaction progress curves of the control were linear over a lengthy period of time. The results analyzed by Zhou and Tsou's method [24] suggested that the Binary union S had a stimulating effect on papain activity, but the Binary union I had an inhibition effect. According to Eq. (1), the exponential linearized expressions had been achieved using least square fitting method by all data in Fig. 3, and the kinetic parameters of the model were shown in Table 3. The results showed that the calculated the correlation coefficients R^2 were greater than 0.974, indicating that the kinetic model could well describe casein hydrolysis during the binary ions binding to papain. According to Eq. (3), the plot of $1/[P_e]$ against $1/[S]$ gave a straight lines. The values of k_0 and k_0' were calculated, and listed in Table 3.

The v value of native papainwas lesser than the v' value of papain exposed in the Binary union S buffer, and this indicated that the Binary union S could stimulate papain catalytic activity. Furthermore, the values of dissociation constant k_0 and k_0' could be obtained, and the ratio of k_0 to k_0' was 0.2954, which suggested that there was a binding of the binary ions (Y) with both the native enzyme (E) and the enzyme-substrate complex (EY), and amount of EYS was more than that of EY. Additionally, a plot of 1/A versus [S] gives a nearly liner ($R^2 = 0.9131$), and A value increased with increasing substrate concentration [S], implying the Binary union S was mainly competitive activator for papain although noncompetitive stimulation also occurred. In our previous work, 10^{-6} mol/L Hg^{2+} was a noncompetitive activator for papain, the binding interactions of Hg^{2+} with papain mainly located outside the active center . Based on the kinetic parameter K_m results (Table S1), the order of the affinity for the substrate was Binary union $S > 10^{-9}$ mol/L $Cu^{2+} > 10^{-6}$ mol/L $Hg^{2+} > 10^{-4}$ mol/L

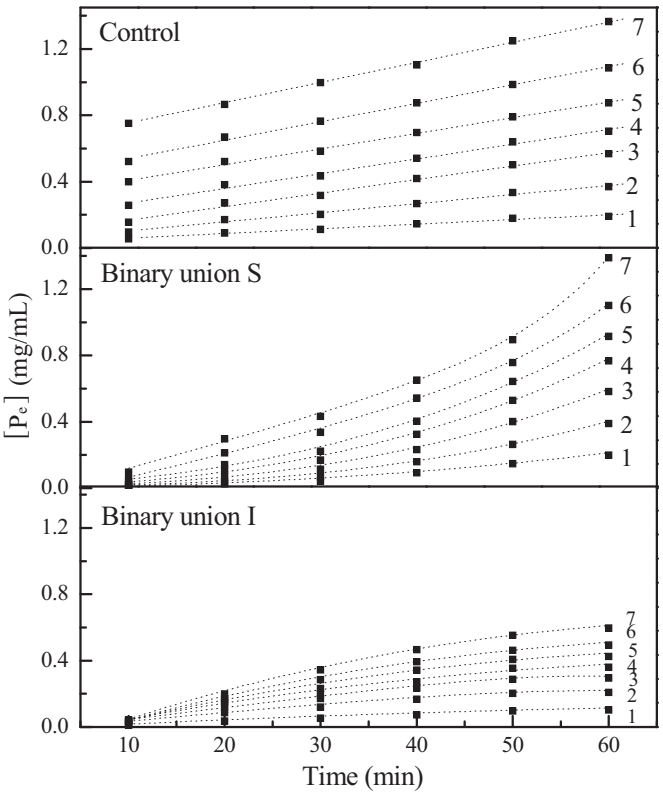

Fig.3. Time course of casein hydrolysis reaction at different substrate concentrations in the presence of Binary union S and I buffer. (1) 0.2 mg/mL casein; (2) 0.4 mg/mL casein; (3) 0.6 mg/mL casein; (4) 0.8 mg/mL casein; (5) 1.0 mg/mL casein; (6) 1.4 mg/mL casein; (7) 2.0 mg/mL casein. ·····: Prediction; ■: experiment.

Table 3
Kinetic parameters and dissociation constant of papain samples at the two Binary union S and I combinations.

No.	Casein concentration (mg/mL)	A (mg/mL)	v' (mg/min)	V (mg/min)	$[P_e]$ (mg/mL)	R^2	k_0	k_0'
Control	0.2	–	0.0028	0.0028	0.1984	0.987		
	0.4	–	0.00549	0.00549	0.3908	0.990		
	0.6	–	0.00815	0.00815	0.5809	0.992		
	0.8	–	0.00889	0.00889	0.7082	0.992	–	–
	1.0	–	0.00944	0.00944	0.8687	0.996		
	1.4	–	0.01111	0.01111	1.0824	0.996		
	2.0	–	0.01211	0.01211	1.3465	0.999		
Binary union I	0.2	0.00863	0.00176	0.00664	0.1135	0.987		
	0.4	0.05267	0.00594	0.00683	0.2195	0.989		
	0.6	0.07716	0.00756	0.00978	0.3066	0.992		
	0.8	0.00850	0.01075	0.03342	0.4394	0.974	0.114	5.493
	1.0	0.00673	0.02118	0.05733	0.6078	0.985		
	1.4	0.00858	0.01913	0.05619	0.7070	0.996		
	2.0	0.00752	0.02677	0.07482	0.8423	0.993		
Binary union S	0.2	0.01222	0.00469	0.00106	0.1987	0.986		
	0.4	0.01499	0.01097	0.00023	0.3936	0.994		
	0.6	0.01647	0.0131	0.00026	0.5883	0.994		
	0.8	0.01852	0.0113	0.00203	0.7243	0.996	0.688	2.329
	1.0	0.01834	0.01181	0.00313	0.8927	0.997		
	1.4	0.07880	0.01347	0.00667	1.1022	0.998		
	2.0	0.11128	0.01604	0.01017	1.3871	0.998		

The reactions were performed at 40 °C, pH 7.0 for 30 min, 1.0 mg/mL papain Tris–HCl solution in different concentration combinations of Hg^{2+} and Cu^{2+} ions. Every group test was run three times and the mean values were used as the final test results.

$Cu^{2+} \approx$ Binary union I $> 10^{-4}$ mol/L Hg^{2+}. In the Binary union S buffer, papain had two sites of combination for the activator, one in the active pocket and the other one on the surface of enzyme. Since Cu^{2+} had higher affinity to papain, it may insert into the active pocket, while Hg^{2+} bond with the binding site of the surface to some extent. The binding of Binary union *S* to papain induced papain conformation to change especially due to the decrease of intermolecular β-sheet aggregates content (Table 2), so that the hydrophobic pocket became bigger. It could be hypothesized that the combination of the substrate with the enzyme molecule induced a broadened hydrophobic pocket in the enzyme-substrate complex, and the combination of the substrate with papain molecule would be easier to engender, leading the increase of papain activity.

The v value was higher than the v' value in the Binary union I buffer, revealing that the Binary union I was an inhibitor for papain. The ratio of k_0 to k_0' was 1.8028, showing that binding of the Binary union I with papain also had two existing form, EY and EYS, but the amount of EY was more than that of EYS. The apparent rate constant A was independent from [S] (Table 3), namely the inhibition had nothing to do with the substrate concentration, implying that the Binary union I was noncompetitive inhibitor for papain and could bind with papain at the active sites both in the active pocket and on the protein surface. Results from those experiments ranged from inhibitory to synergistic responses (Tables 1 and 3), though the overall trend was for Cu^{2+} to reduce toxicities of Hg^{2+} on papain. The negative interaction between Cu^{2+} and Hg^{2+} was probably the result of the competition between Cu^{2+} and Hg^{2+} at the binding sites of papain.

As described in our previous work (data not shown), 10^{-4} mol/L Hg^{2+} as competitive inhibitor was found to mainly bind at the active sites in papain active pocket. Since Hg^{2+} was a typical soft acid, and papain was one of cysteine proteinases should contain soft bases, i.e., cysteine residues, Hg^{2+} had a strong bind with the residues resulting in almost full deactivation of papain. The inhibition of Hg^{2+} could be recovered in the presence of Cu^{2+} (Table S1). Cu^{2+} with higher affinity for papain could recover papain activity by competitively binding to the active sites, which leading to the decrease of the inactive sites for Hg^{2+}. It was speculated that the active sites should favor small metal ions. Since Hg^{2+} had a much larger radius than Cu^{2+}, it was reasonable that Hg^{2+} might deviate from the metal binding sites of papain and therefore much less effective than Cu^{2+} in the inhibiting effect.

4. Conclusion

The study demonstrated that there were significant impacts of the binary ions (Hg^{2+} & Cu^{2+}) on papain. The strongest inhibitive effect was observed when Hg^{2+} and Cu^{2+} concentration was up to 10^{-4} mol/L, whereas maximum activation concentration was 10^{-8} mol/L Cu^{2+} + 10^{-6} mol/L Hg^{2+}. So, the low detection limit for papain was 10^{-4} mol/L concentration of Hg^{2+} + Cu^{2+}. The results showed that the performance of papain was suitable for the quantitative determination of the binary ions in environmental analysis.

The fundamental correlations between the structure of papain and its catalytic activity were clarified. The three-dimensional structure of the papain exposed in the binary ions was determined by ATR-FTIR, UV–vis and fluorescence spectroscopies. The papain exposed in the Binary union S buffer had increase in α-helix content and decrease in intermolecular β-sheet aggregates content, but the papain exposed in the Binary union I buffer had increase in intermolecular β-sheet aggregates but decrease in α-helix content. The papain activity increased with the increase of α-helix content and decrease of intermolecular β-sheet aggregates content, and vice versa.

More experimentation was necessary to better understand the mechanisms underlying the interactions between heavy metals such as Hg^{2+} & Cu^{2+}, and it was evident that the interactions of the binary ions affected papain activity considerably. There were difference interaction mechanisms between the binary ions and single Hg^{2+}. The Binary union S as a competitive stimulator was better able to enhance papain activity than single Hg^{2+} at 10^{-6} mol/L or Cu^{2+} at 10^{-9} mol/L. For single Hg^{2+}, the Hg^{2+} at 10^{-4} mol/L was a competitive inhibitor and papain activity was almost lost completely, suggesting that the SH group situated at the active site in active packet of papain was essential to maintain its catalytic activity and the reaction of Hg^{2+} with SH group led the enzyme activity to lose entirely. However, the inhibition of papain by the binary ions in the Binary union I buffer belonged to be noncompetitive type. Cu^{2+} bonded preferentially with papain into the active packet by removing Hg^{2+} leading to the mostly binding of Hg^{2+} with the cysteine

residues (SH group) outside of papain active packet. Regardless of being inhibition or stimulation, the overall trend was for Cu^{2+} to block the inhibitive effect of Hg^{2+} on papain. In higher binary ions concentration, the recovery of papain activity should be due to removal of Hg^{2+} by the superiorly competitive ligands of Cu^{2+} and the active sites of papain.

Acknowledgments

This work was supported by National Natural Science Foundation of China (21105085, 31270988), Hunan Provincial Natural Science Foundation of China (No. 2015JJ2133), Scientific Research Fund of Hunan Provincial Education Department (13B120) and Economical Forest Cultivation and Utilization of 2011 Collaborative Innovation Center in Hunan Province [(2013) 448].

Appendix A. Supplementary data

Supplementary data associated with this article can be found, in the online version, at http://dx.doi.org/10.1016/j.bej.2015.01.001.

References

[1] A. Amine, H. Mohammadi, I. Bourais, G. Palleschi, Biosens. Bioelectron. 21 (8) (2006) 1405–1423.
[2] A.L. Ghindilis, P. Atanasov, E. Wilkins, Electroanalytical 9 (9) (1997) 661–674.
[3] M.R. Guascito, C. Malitesta, E. Mazzotta, A. Turco, Sen. Actuators B: Chem. 131 (2) (2008) 394–402.
[4] C. Guo, J. Wang, J. Cheng, Z. Dai, Biosens. Bioelectron. 36 (1) (2012) 69–74.
[5] Y. Guo, Z. Wang, W. Qu, H. Shao, X. Jiang, Biosens. Bioelectron. 26 (10) (2011) 4064–4069.
[6] S.S. Husain, G. Lowe, Biochem. J. 114 (2) (1969) 279–288.
[7] C.M. Jonsson, L.C. Paraiba, H. Aoyama, Ecotoxicology 18 (5) (2009) 610–619.
[8] T.J. Kamerzell, R. Esfandiary, S.B. Joshi, C.R. Middaugh, D.B. Volkin, Adv. Drug Deliv. Rev. 63 (13) (2011) 1118–1159.
[9] I.G. Kamphuis, K.H. Kalk, M.B.A. Swarte, J. Drenth, J. Mol. Biol. 179 (2) (1984) 233–256.
[10] J. Kong, S. Yu, Acta Biochim. Biophys. Sin. 39 (8) (2007) 549–559.
[11] T. Krawczyński vel Krawczyk, M. Moszczyńska, M. Trojanowicz, Biosens. Bioelectron. 15 (11–12) (2000) 681–691.
[12] F. Kuralay, H. Özyörük, A. Yıldız, Enzyme Microb. Technol. 40 (5) (2007) 1156–1159.
[13] C.R. Llerena-Suster, C. José, S.E. Collins, L.E. Briand, S.R. Morcelle, Process Biochem. 47 (1) (2012) 47–56.
[14] L.H. Lucas, B.A. Ersoy, L.A. Kueltzo, S.B. Joshi, D.T. Brandau, N. Thyagarajapuram, L.J. Peek, C.R. Middaugh, Protein Sci. 15 (10) (2006) 2228–2243.
[15] C. Malitesta, M.R. Guascito, Biosens. Bioelectron. 20 (8) (2005) 1643–1647.
[16] H.-L. Nie, T.-X. Chen, L.-M. Zhu, Sep. Purif. Technol. 57 (1) (2007) 121–125.
[17] P.R. Palaniappan, V. Vijayasundaram, Infrared Phys. Technol. 52 (1) (2009) 32–36.
[18] W.P. Richard, R. Pierre, W.H. Gillian, W.G. Peter, Acta Crystallogr. B47 (1991) 766–771.
[19] B. Sharma, S.V. Bykov, S.A. Asher, J. Phys. Chem. B 112 (37) (2008) 11762–11769.
[20] Y. Shukor, N.A. Baharom, F.A. Rahman, M.P. Abdullah, N.A. Shamaan, M.A. Syed, Anal. Chim. Acta 566 (2) (2006) 283–289.
[21] A. Szabó, M. Kotormán, I. Laczkó, L.M. Simon, Process Biochem. 44 (2) (2009) 199–204.
[22] Y. Yang, Z. Wang, M. Yang, M. Guo, Z. Wu, G. Shen, R. Yu, Sens. Actuators B: Chem. 114 (1) (2006) 1–8.
[23] M. Yogavel, N. Nithya, A. Suzuki, Y. Sugiyama, T. Yamane, D. Velmurugan, A. Sharma, Acta Crystallogr. D66 (2010) 1323–1333.
[24] K.-Y. Zhao, C.-L. Tsou, J. Theor. Biol. 157 (4) (1992) 505–521.
[25] X. Zhao, F. Chen, W. Xue, L. Lee, Food Hydrocolloids 22 (4) (2008) 568–575.